Spatial Calibration of Airborne Ultrasound Tactile Display and Projector-Camera System Using Fur Material

Shigo Ko
Keio University.
Yokohama, Hiyoshi 3-14-1, Japan
shigo_ko@imlab.ics.keio.ac.jp

Yuta Itoh
Keio University.
Yokohama, Hiyoshi 3-14-1, Japan
itoh@imlab.ics.keio.ac.jp

Yuta Sugiura
Keio University.
Yokohama, Hiyoshi 3-14-1, Japan
sugiura@imlab.ics.keio.ac.jp

Takayuki Hoshi
The University of Tokyo.
Tokyo, Hongo 7-3-1, Japan
takayuki_hoshi@ipc.i.u-tokyo.ac.jp

Maki Sugimoto
Keio University.
Yokohama, Hiyoshi 3-14-1, Japan
sugimoto@imlab.ics.keio.ac.jp

TEI '17, March 20-23, 2017, Yokohama, Japan
ACM 978-1-4503-4676-4/17/03.
http://dx.doi.org/10.1145/3024969.3025061

Abstract
Airborne Ultrasound Tactile Displays (AUTD) are tactile displays that can generate vibrotactile sensation on human skin. Combining an AUTD with a projector-camera system, it is possible to present synchronous visual and haptic stimuli that is physically aligned in the 3D space. To maintain the synchronous sensation as realistic as possible, an accurate crucial to spatial calibration between the AUTD and the projector-camera system is required. This paper thereby proposes a calibration method for the AUTD system by utilizing fur material to recognize the output focal points of an AUTD in the camera coordinate system. Our method simplifies the calibration procedure with calibration error of 2.63 mm.

Author Keywords
Device Calibration, Airborne Ultrasound Tactile Display, Projector-Camera System

ACM Classification Keywords
H.5.m. Information interfaces and presentation.

Introduction
Airborne ultrasound tactile displays (AUTD) are tactile displays that generate vibrotactile sensations on human

skin[1]. These displays are different from other tactile sensation devices because it can create midair haptic sensation without touching the display devices. By combining an AUTD with a projector-camera system to project images, it is able to produce synchronized visual and tactile stimuli without contact[2]. To combine the AUTD and projector-camera system requires special calibration. There is a remarkable prior calibration method uses a microphone and three-dimensional(3D) stages[3], that requires designated devices, and data collection is time consuming. This research proposes a way to simplify the calibration procedure by using a fur material and recognizing fur fluffing changes to obtain correspondence points between the AUTD and camera image coordinate.

Related Work

There are many haptic devices to produce tactile sensation, such as devices placed on fingertips [8] and a vibration belt on user's waist[9] to produce virtual contents by contact. Also, non-contact devices produce tactile sensation such as air jets[10]. In such research, users must wear or hold devices to perceive the tactile sensation.

AUTD[1] is an ultrasound speaker array that can create an ultrasound focal point in midair. A 3D stage, microphone, and multiple AUTD are used to project an ultrasound to human skin to measure tactile sensation resolution[4]. A user touches a projected image in midair which presents haptic feedback by the AUTD and creates a tactile sensation for the user[5].

Other than producing tactile sensation, AUTD sound pressure distribution was visualized by viscosity fluid visualization[3]. An AUTD was used to draw 2 dimensional pictures by sound pressure stimulus on a fur material [6]. Also, a set of AUTDs controlled floating particles in 3 dimensional space by phased ultrasound waves[7].

Theory

Each device used in this study has an individual coordinate system, including a camera image coordinate P, camera position coordinate C, and AUTD coordinate system W. Corresponding points between each coordinate system are used to calculate transformation matrices corresponding to each device.

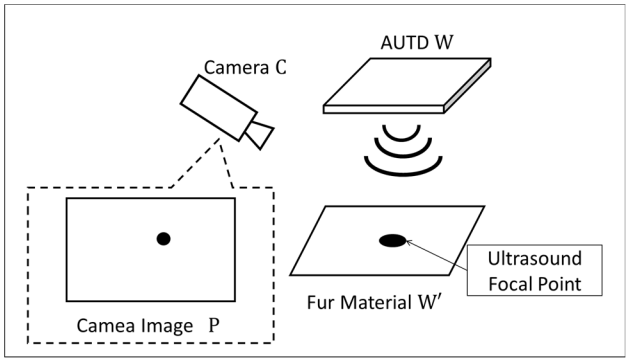

Figure 1: Devices and coordinate systems.

Plane Projective Transformation

Plane projective transformation matrices are calculated to correspond with the planes of the camera coordinate system and AUTD coordinate system. In this study, the transformation of the AUTD coordinate system is obtained as a relative coordinate system from the camera coordinate system. To convert a point in the camera image coordinate system $\boldsymbol{p} = (u, v)$ and plane in the AUTD coordinate system $\boldsymbol{w} = (x'_w, y''_w)$, we use homogeneous coordinates (which is represented as ˜ in

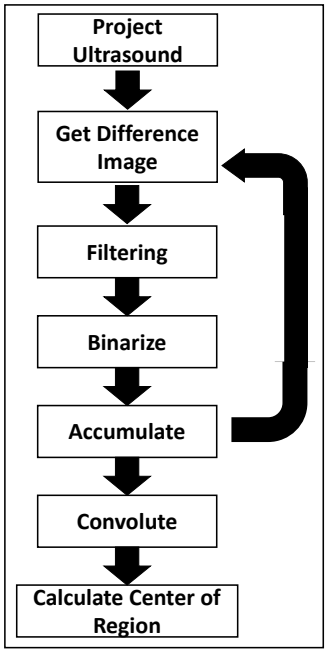

Figure 2: Work flow to recognize the ultrasound focal point.

formulas) and plane projective transformation matrix, $\boldsymbol{H}$ as shown below.

$$\tilde{\boldsymbol{p}} \approx \boldsymbol{H}\tilde{\boldsymbol{w}} \tag{1}$$

$$\Leftrightarrow \begin{bmatrix} u \\ v \\ 1 \end{bmatrix} \approx \begin{bmatrix} h_{11} & h_{12} & h_{13} \\ h_{21} & h_{22} & h_{23} \\ h_{31} & h_{32} & 1 \end{bmatrix} \begin{bmatrix} x_w{}' \\ y_w{}' \\ 1 \end{bmatrix} \tag{2}$$

At least four corresponding point pairs are required to estimate the coefficients of the plane projective transformation matrix. To reduce error more than four pairs of projections point can be used.

Perspective Projection Transformation

The projection matrix is calculated to correspond to the camera 3D coordinate system and AUTD 3D coordinate system and convert points between the AUTD coordinate system $\boldsymbol{W} = (x_w, y_w, z_w)$ and the image coordinate system $\boldsymbol{p} = (u, v)$, which is represented in the following formula.

$$\tilde{\boldsymbol{p}} \approx \boldsymbol{P}\tilde{\boldsymbol{W}} \tag{3}$$

$$\tilde{\boldsymbol{p}} \approx \boldsymbol{K}[\boldsymbol{R}|\boldsymbol{t}]\tilde{\boldsymbol{W}} \tag{4}$$

$$\Leftrightarrow d\begin{bmatrix} u \\ v \\ 1 \end{bmatrix} \approx \begin{bmatrix} f_x & 0 & c_x \\ 0 & f_y & c_y \\ 0 & 0 & 1 \end{bmatrix} [\boldsymbol{R}|\boldsymbol{t}] \begin{bmatrix} x_w \\ y_w \\ z_w \\ 1 \end{bmatrix} \tag{5}$$

$$\Leftrightarrow \begin{bmatrix} x_w \\ y_w \\ z_w \end{bmatrix} \approx \boldsymbol{R}^{-1}\left(\boldsymbol{K}^{-1}\left(d\begin{bmatrix} u \\ v \\ 1 \end{bmatrix}\right) - \boldsymbol{t}\right) \tag{6}$$

$\boldsymbol{K}$	*Matrix of Camera Intrinsic Parameters*
$\boldsymbol{R}$	*Matrix of Rotation*
$\boldsymbol{t}$	*Vector of Translation*
f_x, f_y	*Focal Length*
c_x, c_y	*Center of Image*

Table 1: Parameters of Formulas 4, 5, and 6.

At least six corresponding point pairs of convert points in the image coordinate system to the AUTD coordinate system are required to estimate the coefficients of the perspective projection transformation matrix: the rotation matrix $\boldsymbol{R}$ and translation vector $\boldsymbol{t}$.

Implementation

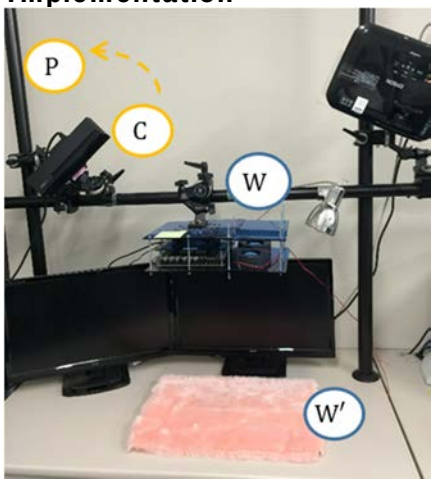

Figure 3: Appearance of the hardware system

The system was consists of an AUTD, camera, projector, and fur material. After placing the fur material under the AUTD, the ultrasound focal point was recognized by changing the fluffing of the fur

Figure 6: An image drawn on fur material using ultrasound projection.

Figure 7: Convolution of the image on the fur material and the image projected from the projector.

material by the ultrasound projected from the AUTD. Figure 2 shows the system flow to recognize the ultrasound focal point. At first, the ultrasound was projected to the fur material to obtain an amplified differential image between the current and previous camera frames(Figure 4). Next, a median filter applied to the differential image to reduce white spike noise in the difference image (Figure 4) then the image was binalized by Otsu's method (Figure 4).

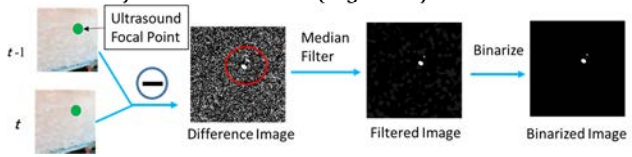

Figure 4: Method to Make Binarized Image

This operation was repeated several times to accumulate output images (Figure 5). To reduce environmental noise, the differential images was convoluted with Non-ultrasound Image using the formula below.

$$\mathrm{P} = \sum_{i}^{n_t} \frac{\mathrm{P}_{ti}}{n_t + n_f} - \sum_{j}^{n_f} \frac{\mathrm{P}_{fj}}{n_t + n_f} \qquad (7)$$

$\boldsymbol{P}$	*Accumulated Image*
$\boldsymbol{P_t}$	*Projected Ultrasound Image*
$\boldsymbol{P_f}$	*Non-ultrasound Image*
$\boldsymbol{n_t}$	*Number of* $\boldsymbol{P_t}$
$\boldsymbol{n_f}$	*Number of* $\boldsymbol{P_f}$

Table 2: Parameters of Formula 7.

The weighted center of the region was calculated from the results of the convoluted image (Figure 5) and used as one of correspondence points to estimate the transformation matrices.

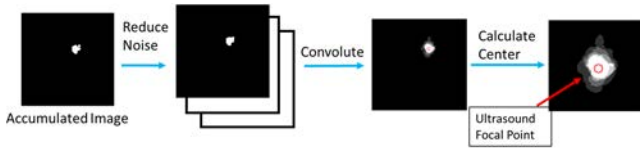

Figure 5: Method to Recognize Ultrasound Focal Point from

Experiment

To evaluate the precision of the ultrasound focal point recognition, we measured the re-projection error of the ultrasound focal points. The distance from the AUTD to the fur material was 450 mm and assumed to be parallel. After calculating the plane projective transformation matrix, the same projection points were converted to points in the image coordinate system by the plane projective transformation matrix from the AUTD coordinate system. The errors between the true point and calculated point were evaluated. Each calculation of the plane projective transformation matrix included nine points and for sets. These results are shown in Table 3. In addition, each point error is shown in Figure 8 and each show error and standard deviation is shown in Figure 9.

Average of error	*2.63mm*
Standard deviation	*1.39mm*

Table 3: Re-projection error of the ultrasound focal point when the plane projective was used.

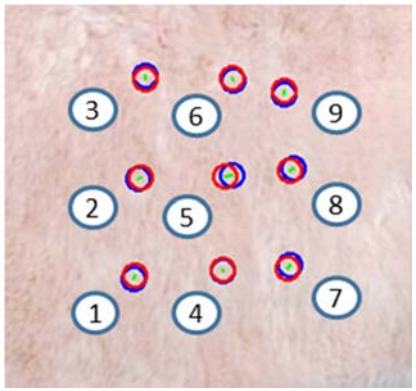

Figure 8: Error of each projection point.

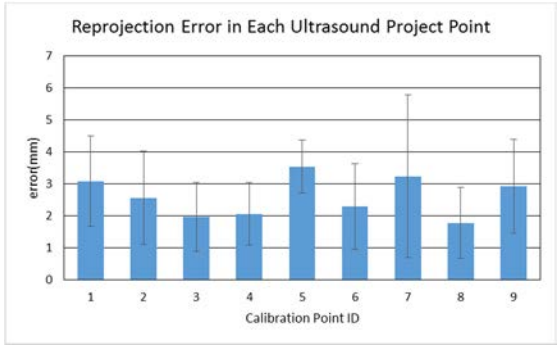

Figure 9: Re-projection error for each ultrasound projection point

Integrate AUTD and Projector-Camera System

By using the transformation matrices between the AUTD-camera and camera-projector coordinate systems, we can convert the AUTD coordinate system to the projector coordinate system (Figure 10). This provides synchronized projected ultrasounds and images by the AUTD-projector conversion model. The calibration result was demonstrated by drawing a static picture on the fur material using ultrasound projection as (Figure 6) and a project image to the static picture (Figure 7).

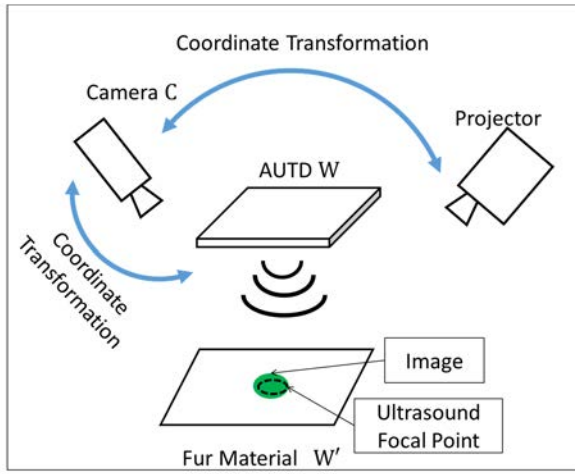

Figure 10: Calibration of the AUTD and projector-camera systems.

Conclusion

In this study, we proposed a method to simplify spatial calibration between the AUTD and projector-camera system. We recognized the ultrasound focal points by obtaining differential images of fluffing changes on the fur material during the ultrasound projection. We combined the AUTD and projector-camera systems using a calibration model for both AUTD-camera and camera-projector systems. In the experiment, the plane projective transformation matrix showed an averaged re-projection error: 2.63 mm as the result of the calibration between AUTD and camera coordinate systems.

Acknowledgements

This work was supported by JSPJ KAKENHI Grant Number 15H01701.

References

1. Takayuki Hoshi et al., Noncontact Tactile Display Based on Radiation Pressure of Airborne Ultrasound, IEEE Transactions on Haptics, pp.155–165, 2010.
2. Kazuma Yoshino et al., Measuring Visio-Tactile threshold for Visio-Tactile Projector, SICE Annual Conference 2012, pp.1996–2000, 2012.
3. Takayuki Hoshi, Visualization of Pressure Distribution of Airborne Ultrasound Tactile Display Utilizing Viscous Fluid, 2013 JSME Conference on Robotics and Mechatronics, 2A2–B04(1–3), 2013.
4. Keisuke Hasegawa et al., Aerial Display of Vibrotactile Sensation with High Spatial-temporal Resolution Using Large-aperture Airborne Ultrasound Phased Array, IEEE World Haptics Conference 2013, pp.31-36, 2013.
5. Yasuaki Monnai et al., Haptomime: Mid-air Haptic Interaction with A Floating Virtual Screen, UIST '14, pp.663–667, 2014.
6. Yuta Sugiura et al., Graffiti Fur: Turning Your Carpet into a Computer Display, UIST'14, pp.149–156, 2014.
7. Yoichi Ochiai et al., Pixie Dust: Graphics Generated by Levitated and Animated Objects in Computational Acoustic-potential Field, SIGGRAPH 2014, Article No. 85, pp.1–13, 2014.
8. Kouta Minamizawa et al., Gravity Grabber: Wearable Haptic Display to Present Virtualmass Sensation, ACM SIGGRAPH 2007 Emerging Technologies, Article No. 8, 2007.
9. Robert W. Lindeman et al., Wearable Vibrotactile Systems for Virtual Contact and Information Display, VirtualReality, pp.203-213, 2006.
10. James C. Gwilliam et al., Design and Control of an Air-jet Lump Display, IEEE haptics Symposium 2012, pp.45-49, 2012.